ORNL/TM-2021/2216

Thermal Property Characterization of Molten Salt Reactor–Relevant Salts

N. Dianne Bull Ezell
Ryan C. Gallagher
Can Agca
Jake McMurray

September 2021

Approved for public release.
Distribution is unlimited.

OAK RIDGE National Laboratory

ORNL IS MANAGED BY UT-BATTELLE LLC FOR THE US DEPARTMENT OF ENERGY

ORNL/TM-2021/2216

Nuclear Energy and Fuel Cycle Division
Materials Science and Technology Division

Thermal Property Characterization of Molten Salt Reactor–Relevant Salts

N. Dianne Bull Ezell
Ryan Gallagher
Can Agca
Jake McMurray

September 2021

Prepared by
OAK RIDGE NATIONAL LABORATORY
Oak Ridge, TN 37831-6283
managed by
UT-Battelle LLC
for the
US DEPARTMENT OF ENERGY
under contract DE-AC05-00OR22725

CONTENTS

LIST OF FIGURES

ACKNOWLEDGMENTS

This work is funded by the US Department of Energy's Office of Nuclear Energy Molten Salt Reactor (MSR) Campaign under the Advanced Reactor Technology (ART) program. The authors would like to thank Nick Russell, Paul Rose, Alex Martin, Abbey McAlister, and Shay Chapel for their efforts on this project.

1. INTRODUCTION

The thermochemical and thermophysical properties of molten salt systems are necessary input for the design, licensing, and deployment of molten salt reactor concepts. The thermochemical and thermophysical property measurement capabilities being used and developed at Oak Ridge National Laboratory (ORNL) include liquid density, volumetric thermal expansion, viscosity, vapor pressure, phase behavior, and heat capacity and thermal conductivity measurement capabilities.

Properties of eutectic LiF-NaF-KF (FLiNaK) and NaCl-KCl are being measured to validate the measurement techniques to be used to provide data to reactor developers and to better quantify the uncertainty of measurements. This report summarizes the status of thermal conductivity, viscosity, specific heat capacity, and density. A method for property estimation using Redlich Kister expansion is also described. This technique will be used to help validate measured properties and to guide future experiments by targeting mixtures or components for which data are uncertain or lacking.

2. CHARACTERIZATION CAPABILITIES AT ORNL

Oak Ridge National Laboratory focused on development of technologies for four core capabilities: thermal conductivity, density, viscosity, specific heat capacity.

2.1 Sample Preparation and Characterization

The purity of molten salt samples must be characterized prior to analysis, because impurities have been linked to increased corrosion rates and may lead to biased measurements in some molten salt mixtures. Therefore, purification and compositional characterization is necessary prior to experimental property evaluation.The FLiNaK analyzed in this work was purified by hydroflourination completed by Electrochemical Systems Inc. (ECS) using procedures developed at Oak Ridge National Laboratory (2). As noted by Sulejmanovic et al., previous corrosion tests and inductively coupled plasma (ICP) optical emission spectroscopy (OES) analysis on a sample from this batch indicated low levels of impurities (3; 4).

The salt sample used in these measurements was characterized though combustion analysis on two LECO ONH-836 instruments, oxygen hot extraction, ICP mass spectroscopy (MS) on a Thermo-Finnigan Element 2 instrument, glow discharge mass spectroscopy, and capsule corrosion experiments. Additional detail on the salt characterization can be found in the literature (3). The salt samples used in the measurements discussed in the following sections were prepared and stored in argon gloveboxes at 0.4 ppm oxygen and 0.1 moisture levels or lower. Preparation included loading salt into the experiment crucibles and sealing inside Ar vials for transport to the instruments, when necessary. In the case of the density measurement system described herein, the full apparatus is located inside an Ar glovebox. Thermal conductivity and viscosity cantonments are sealed while in the glovebox.

2.2 Thermal Conductivity - Variable Gap System

The variable gap thermal conductivity system was used to measure the thermal conductivity of molten salts. In the previous fiscal year (FY), the technique was validated up to 500 °C on helium gas and a commercially available nitrate salt. It was determined that axial heat losses resulted in erroneously high

thermal conductivity measurements at temperatures exceeding 500 °C, but the results were adequate to validate the technique. However, the measurement of higher temperature salt mixtures required modifications to the instrument.

In FY21, the variable gap system was modified and rebuilt with alloy C-276 components to reduce corrosion with various molten salt specimens, including chloride and fluoride molten salts. An axial guard heater was also added to the system to prevent axial heat losses, extending the operating range above 900 °C. Experiments were completed using FLiNaK molten salt. An image of the apparatus and the measured apparent thermal conductivity of FLiNaK are shown in Figure 1, with comparison to literature data. The apparent thermal conductivity is listed because the thermal radiation interactions are not corrected for in these data. Molten salts are expected to participate in thermal radiation heat transfer. Therefore, optical properties (including refractive indices and coefficients of absorption) are necessary to fully correct for the effects of these phenomena on the measured conductivity. A correction for this system is currently under development. It is noted that the measured thermal conductivity is weakly dependent on temperature, except at temperatures above 700 °C. This indicates that the convection, heat losses, and radiative heat transfer effects are not substantially impacting the measured values. At the higher temperature range, a stronger positive temperature dependence is observed, potentially owing to a larger radiative heat flux magnitude which was not accounted for during the data analysis. It is possible that a radiation correction would eliminate this positive dependence.

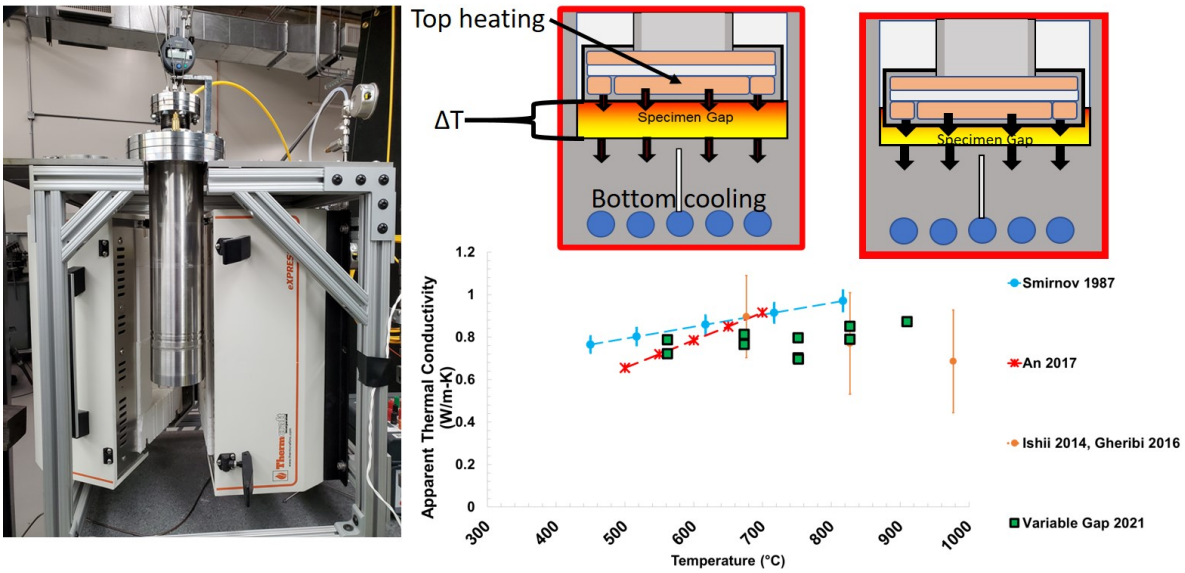

Figure 1. The variable gap thermal conductivity system (left) and the measured apparent thermal conductivity of FLiNaK.

Previous experimental results using laser flash from An et al. (5) and coaxial cylinders from Smirnov et al. (6) show positive temperature dependencies. These results are in disagreement with molecular dynamic simulations and theory (7; 8). It is expected that convective, radiative, or heat loss errors influenced the previous experimental measurements; therefore, the techniques employed by An et al. and Smirnov et al. have been excluded from critically reviewed reference data sets (9). The comparison with literature and the examination of data suggest that optical properties will be necessary for development of reliable heat transfer models of molten salt systems and for accurate measurement of thermal conductivity or diffusivity.

2.3 Density - Archimedes Bob

The displacement technique, or Archimedes method, has been widely applied to determine the densities of liquids and solids and is an accepted technique for molten salt. The weight of a solid plummet as measured in a known gas is compared to the weight while submerged in the fluid sample being measured. The force applied on the plummet while submerged is equal to the weight of the displaced liquid. Therefore, the density of the fluid can be determined by dividing the weight difference over the volume of the plummet. At high temperatures, Eq. (1) is used to correct for the effects of the plummet's thermal expansion, as well the surface tension force exerted on the suspension wire by the fluid (5; 10; 11):

$$\rho_{fluid} = \frac{\omega_0 - \omega_{fluid} + \frac{\pi D \sigma cos(\theta)}{g}}{V[1 + a(T - T_{ref})]^3}, \tag{1}$$

where ω_0 is the weight of the plummet outside of the fluid, ω_{fluid} is the weight of the plummet measured while submerged in the fluid, D is the diameter of the suspension wire, σ is the surface tension of the fluid, θ is the contact angle, V is the volume of the plummet, T is the temperature of the fluid, a is the coefficient of thermal expansion (CTE) of platinum, T_{ref} is the reference temperature of the CTE, and g is gravitational acceleration.

The surface tension correction depends on the wetting properties of the wire and can exert forces with or against the direction of gravity, depending on the wire-fluid contact angle (11). Molten salts generally exhibit hydrophilic behavior on metallic surfaces, so they would have contact angles $\angle 90°$ and would exert a force in the direction of gravity. In practice, the surface tension effect has been assumed to be near zero for molten salt measurements, which would correspond with complete wetting. However, contact angles would be dependent on the material and surface roughness of the wire, so additional consideration may be necessary when correcting for the surface tension effect. Given the weight of the plummet and the diameter of the wire in the setup used in this work, the impact of a contact angle between 0–90 ° results in relatively small error.

The apparatus was built and installed in an argon glovebox at ORNL. The current system employs a platinum plummet suspended from the bottom of a precision balance by a thin metal wire (Ni, stainless steel, or Inconel). The balance is located on a stand above the glovebox's thermal well, which contains a three-zone tube furnace. The thermal well is cooled by recirculating chilled water lines on its outside surface. These chilled water lines maintain the glovebox at an adequate operating temperature while the furnace is running. The specimen is contained within a cylindrical 316 stainless-steel crucible which holds the specimen at the furnace's axial midplane, where the temperature is the most temporally stable and axially uniform. Figure 2a shows the density apparatus when operated outside the glovebox's thermal well.

Density measurements of FLiNaK were made at incremental temperatures starting at 470°C after being held for 15 minutes above the melting point to let the salt homogenize. Measurements started once the mass fluctuation on the balance was less than 0.5 mg. Four separate weight measurement were recorded at each temperature point separated by approximately 15 minutes. The average value of the four measurements and the uncertainties calculated via propagation of errors are listed on Figure 2b with an assumed contact angle of zero. These results agree well with those found by Rose et al. (12), Cheng et al.(10), and An et al.(5), which also feature surface tension corrections. The results are also similar to those of Cohen and Jones (13), which include a cited uncertainty of 5%. Cibulkova(14) and Chrenkova(15)

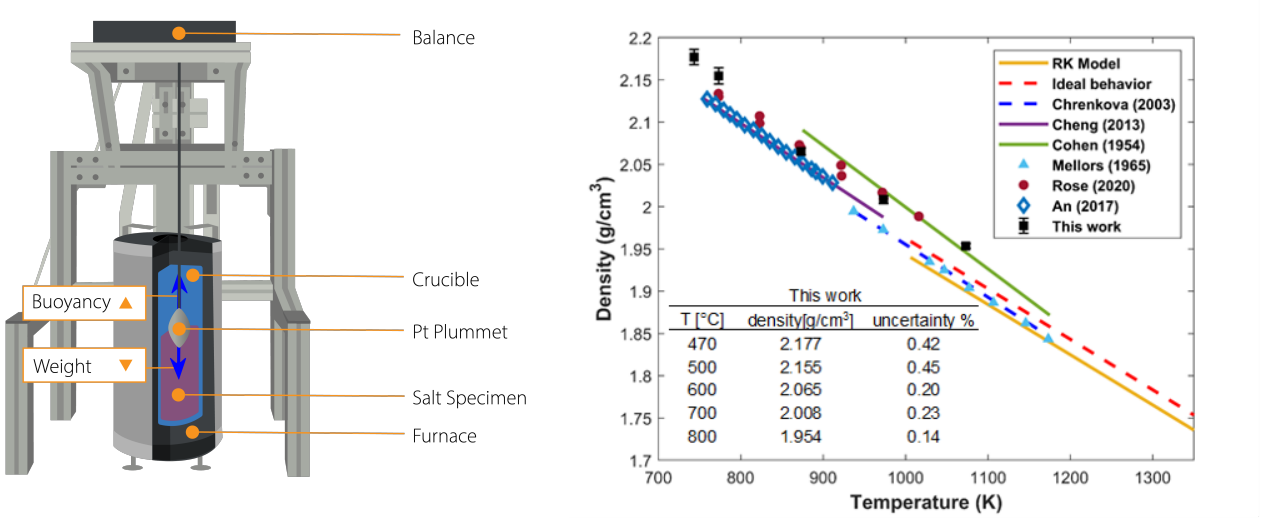

(a) **(b)**

Figure 2. (a) Illustration of density system and (b) density data for FLiNaK salts.

results align well with data from Mellors et al. (16), but they do not feature corrections for surface tension. Furthermore, the Mellors data, as referenced in the Janz and Tomkins' database (17), have an uncertainty of 2%. This uncertainty covers the majority of the other works. The noted differences between experimental data sets may also be small enough to be caused by effects of contact angles, assumed thermal expansion coefficient, and salt composition. The major source of uncertainty was the balance instability, which was as high as 0.02 g, despite having a calibrated accuracy of 0.1 mg. Uncertainties were largest near the lower temperatures, which may have been caused by non-equilibrium conditions in the salt or glovebox. Therefore, these lower temperature points may require re-examination. These results had a maximum measurement uncertainty of <0.5%. Given the agreement with Rose et al. (12), especially between 600–800°C, it is suggested that these values can be used as reference quality data.

2.4 Viscosity - X-Ray Falling Ball

A system was designed to measure the viscosity of molten salts up to 1,000 °C using an adaptation of the falling ball viscosity measurement method. The technique uses x-ray radiography to collect images of a ball falling through a fluid inside of a metal tube which is heated inside a clam shell furnace. The use of metal as the tube material allows for measurement of salts that are not compatible with glass, like most fluoride salts. Tighter machining tolerances are also achievable with with metal components. This enables viscosity measurements of low (<1 Cp) viscosity salts like chloride salts at higher operating temperatures of 700°C and above. The system is shown in Figure 3.

Modifications were made to the system described previously (18). The main upgrade included the addition of custom crucibles that can accommodate repeated drops at a given temperature. This greatly reduced the statistical uncertainty caused by the limited number of drops performed at each temperature point. The crucible is comprised of a larger diameter section near the top and bottom with a smaller diameter section in the middle. The larger sections are offset from the axis of the middle section, creating a step/ledge at the

point where the tubes are joined. During the measurement procedure, the ball is located on the ledge until thermal equilibrium is reached. Then, the tube is rotated 180° around its cylindrical axis, which releases the ball into the middle section.

The middle section has a tightly controlled inner diameter which reduces errors that result from non-uniformities in the tube. Measurements of the ball's descent are taken in this portion of the tube. After the ball has fully descended, the entire furnace is tilted to return the ball to the top section for additional measurements. The custom crucibles are designed to be loaded and sealed inside a glove box and transported to the system for measurement, thus ensuring a high purity environment during testing.

Viscosity measurements rely on measuring the fall time or terminal velocity in previously calibrated pairings of tubes and balls. This FY's successful calibration of viscosity tubes was completed using the radiography setup. Three National Institute of Standards and Technologies (NIST)-traceable standards were used to calculate the calibration coefficient using multiple trials. Then a calibration coefficient was calculated from the trials and used to calculate the viscosity over all of the trials. The results of measurements based on the viscosity standards and examples of the radiographs are shown in Fig. 3 b. The viscosity of these fluids spans the typical range for molten salts at prototypical reactor operating conditions, demonstrating that the technique should be adequate for use with a variety of molten salts. Efforts to measure molten salts with the developed system are currently ongoing at this writing. Unexpected delays during the fabrication of the custom tubes, which required re-working and modification upon arrival, led to delays in molten salt measurement.

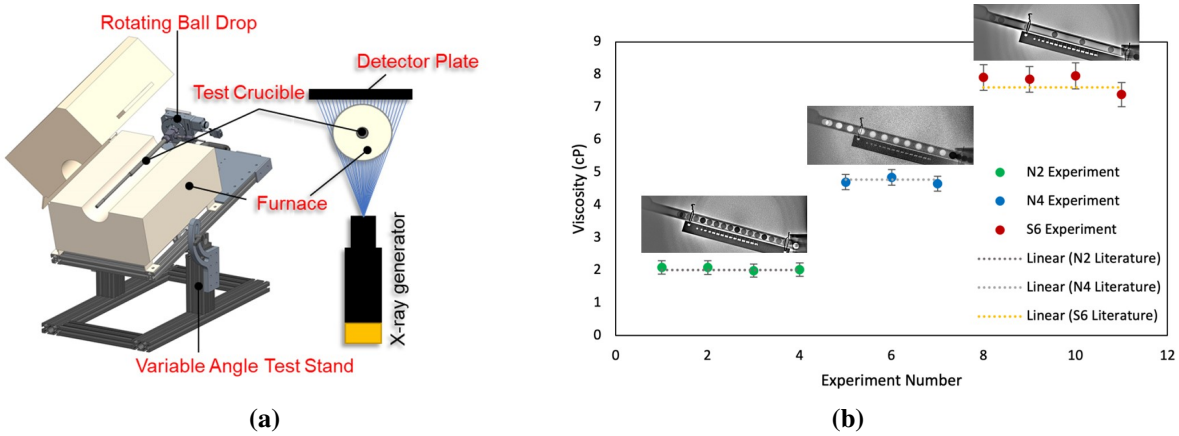

Figure 3. (a) Diagram of the x-ray falling ball viscosity system, and (b) measured data with correlated x-ray images.

2.5 Specific Heat Capacity - Differential Scanning Calorimetry

Heat flux differential scanning calorimetry (DSC) was used to measure the specific heat of FLiNaK. The technique uses two thermocouples that measure the temperature difference between a sample and a reference resulting from dynamic heating according to Boettinger et al. [2007]. The thermocouples are coupled by a heat flow path of well-defined geometry and thermal properties (i.e., thermal conductivity and specific heat). This allows the temperature differences to be correlated to heat flow via mathematical formalisms to yield quantitative specific heat data.

Measurements were performed using a Pegasus 404C DSC from Netzsch Gerätebau GmbH (Selb, Germany). This commercially available system was calibrated by the manufacturer. The crucible was fabricated out of glassy carbon with a gravity sealed lid. Glassy carbon was selected for its low surface free energy, which limits the influence of wetting on a measurement. The crucible was separated from the Pt stage by an alumina diffusion barrier to prevent dissolution of C into the Pt, a reaction that would produce or consume heat energy and cause inaccurate results.

An empty sample crucible and an empty reference crucible were subjected to a series of runs to establish a repeatable background, with the same temperature program chosen for each subsequent run. The specific heat of the sample was then measured to provide calibration data. The FLiNaK was ground using a mortar and pestle in an argon glove box and was loaded into the empty sample crucible. The measurement was repeated with the reference crucible present. Airgas flowing at 100 cc/min passed over hot Cu at 650 °C to bring residual impurities such as O_2, H_2O, and other oxygen-bearing vapor species to sub ppm levels. The heating rate was 10 °C/min from room temperature to 800 °C.

The results of the heat capacity measurements on FLiNaK are shown in Figure 4 in comparison with previous experimental data (19), as well as predicted heat capacity using ab-initio molecular dynamics (AIMD), classical molecular dynamics (MD), the Molten Salt Thermodynamic Data Base (MSTDB-TC) (20), and the Neumann-Kopp rule. Differences are evident in the two different trials, one of which measured a higher heat capacity relative to the estimates and which has a positive temperature dependence and relatively high noise. This trial was completed after a full heat-up and cool-down cycle was run in the DSC. It is possible that vaporization may have influenced this set of data. The other set was measured on the initial heating cycle and showed reasonable agreement with predicted values, but an unexpected negative temperature trend. The data are currently under investigation to determine the causes of the observed behavior. It is clear that the preparation and procedure for measuring molten salts is a major source of error and should be carefully considered and documented when making these measurements.

Tests with NaCl-KCl were completed in a simultaneous thermal analyzer (STA) to determine the adequacy of the glassy carbon crucibles for containing chloride salts. However, mass losses were measured before and after heating, disqualifying this crucible for use in the DSC with chloride salts. Alternatively, a custom crucible featuring an electron beam sealed lid is being developed at ORNL to enable measurements with volatiles of highly wetting molten salts. The crucible design is shown in Figure 5.

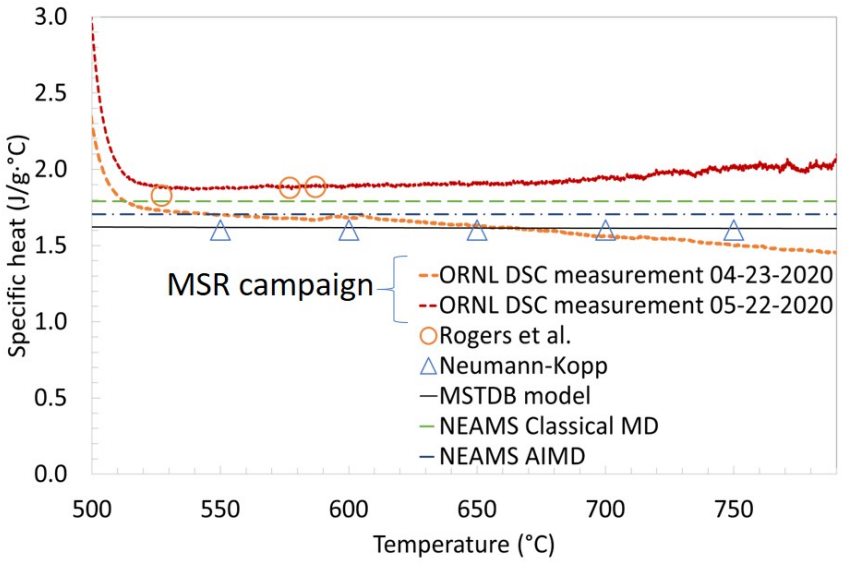

Figure 4. Heat capacity data

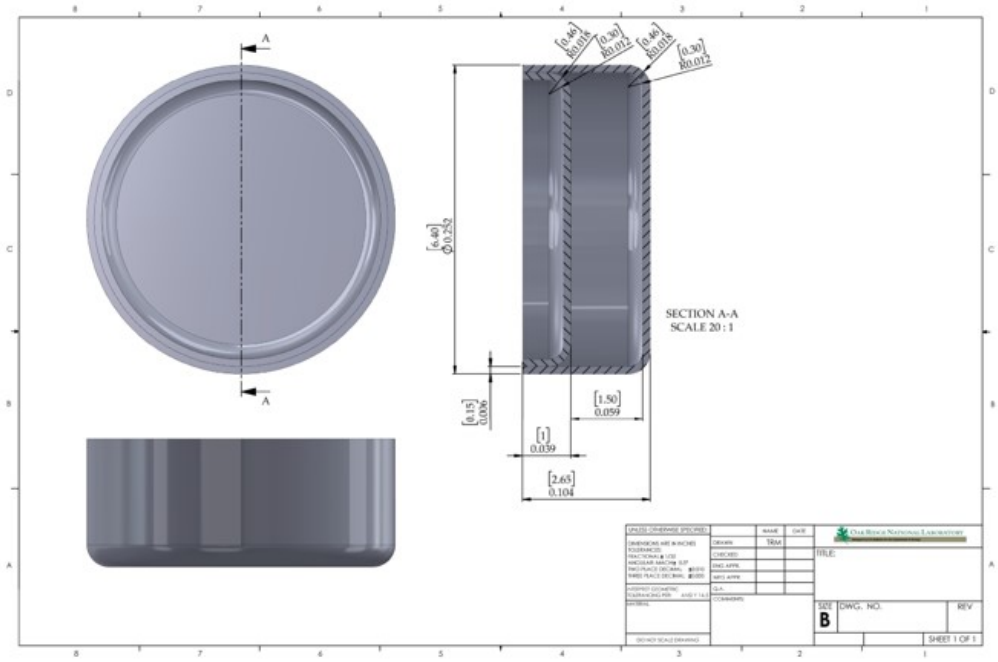

Figure 5. Custom crucible design at ORNL for DSC measurements. Rh, Au, and weldable Mo are the materials of choice

.

3. MODELING TO ASSIST THE CHARACTERIZATIONS

The thermophysical properties measurement techniques outlined here can be assisted by thermophysical modeling, which is a useful tool in the estimation of density, viscosity, and thermal conductivity of multicomponent molten salts (21; 20). In the modeling procedure, the experimental reference data are collected and critically assessed. Then, the data for pseudobinary molten salt systems are used to obtain a relation that is a function of temperature and composition. The Redlich-Kister (RK) expansion (22) is used in the thermophysical modeling of molten phases. It requires pure liquid properties as a function of temperature and reference data at different compositions against which to model. Estimation of density is provided as an example here. Equation 2 calculates the density of the mixture at the desired composition and temperature:

$$\rho_{mix} = \frac{x_A MW_A + x_B MW_B}{\frac{x_A MW_A}{\rho_A} + \frac{x_B MW_B}{\rho_B}} + x_A x_B \sum_{j=1}^{n} L_j (x_A - x_B)^{j-1} \tag{2}$$

$$L_j = A_j + B_j T \tag{3}$$

The first part of Eq. 2 is the density of liquid mixture that behaves ideally. It is simply the ratio of the molar mass to the molar volume. Pure molten salt density, ρ_i, and molecular weight of the salt, MW_i are required to calculate the ideal behavior density of the mixture. The L_j term is an RK binary interaction parameter which accounts for the non-ideal behavior of the density of the mixture. All temperature units are in Kelvin. The RK formalism is commonly used in the CALPHAD (Computer Coupling of Phase Diagrams and Thermochemistry) method to describe excess Gibbs free energies (23). The $j - th$ order of the interaction parameter can be increased to enhance the fit and to model the multi-body interactions in the binary system. To model the density at different temperatures, L_j is defined as a linear function of temperature, as in Eq. (3). The $LiF - ThF_4$ molten salt system density model is shown in Figure 6. There is a good agreement within 2% of the reference data (1). The system exhibits ideal behavior at low temperatures and shows negative deviation above 1,300 K.

The binary interaction parameters can be used to extrapolate to ternary and higher order (multicomponent) systems. In thermodynamics of the materials, the multicomponent system behavior can be estimated by extrapolation from the lower order systems. Therefore, the unary and binary system properties are fundamental. The fact that two species interactions generally dominate for the system property has been demonstrated (24; 25; 26; 27). The same strategy can be used for extrapolating to thermophysical properties of multicomponent systems. The Muggianu interpolation can be used to extrapolate the density of ternary or higher order systems with binary interaction parameters (23), (28). For a ternary system with Muggianu interpolation, the non-ideal density part is composed of three binary interaction parameters, as shown in Eq. (4).

$$\rho_{ex} = x_A x_B \sum_{j=1}^{n} L_j (x_A - x_B)^{j-1} + x_A x_C \sum_{j=1}^{n} L_j (x_A - x_C)^{j-1} + x_B x_C \sum_{j=1}^{n} L_j (x_B - x_C)^{j-1}. \tag{4}$$

The extrapolation from the binaries strategy is currently in progress and will be presented in a series publication. However, the modeling outlined here indicates that the pure thermophysical property data are the backbone of these calculations. Even if there is no pseudobinary molten salt data, one can estimate

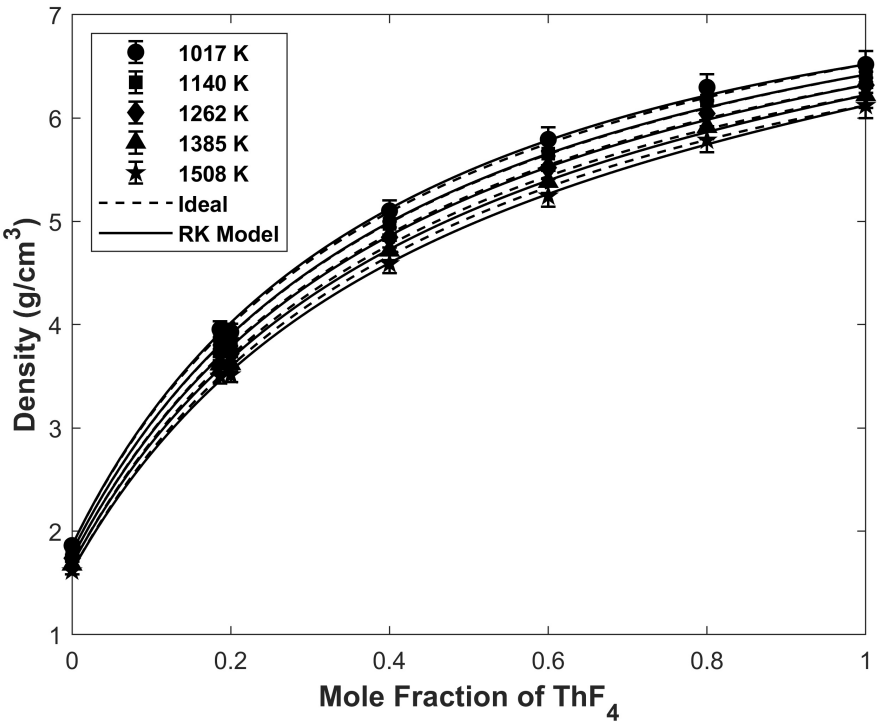

Figure 6. Modeled density of LiF-ThF4 molten salts using RK model and ideal behavior assumption. Reference data from Hill et al. (1). Error bars show 2 % uncertainty range.

density, viscosity, thermal conductivity, and heat capacity simply by assuming ideal behavior. The status of the thermophysical properties of molten salts relevant to the MSR campaign are given in Figures 7–8. The density, heat capacity, and viscosity of the pure molten salts are mostly available, whereas the thermal conductivity of the salts are either contradicting or missing. High quality measurements are needed for contradicting and missing properties to allow for a thorough understanding of thermophysical properties. Furthermore, it can be seen that the fluorides (Figure 8) have more missing data. This can be attributed to their high melting temperature, which makes it difficult to measure the properties. A solid experiment is required to fill the voids of pure molten salt properties in these figures.

Salt	Density	Viscosity	Thermal conductivity	Heat Capacity	Melting T (°C)
$AlCl_3$					610
$BaCl_2$					962
$CeCl_3$					822
$CeCl_4$					-
$CrCl_2$					824
$CrCl_3$					1152
CsCl					645
$FeCl_2$					677
$GdCl_3$					602
KCl					770
LiCl					610
$MgCl_2$					714
NaCl					801
$NdCl_3$					758
$NiCl_2$					1030
$PuCl_3$					767
$SrCl_2$					873
$ThCl_4$					770
UCl_3					841
UCl_4					590
$ZrCl_4$					437
CsI					634

* **Green:** Experimentally supported or well-established; **Yellow:** Only theoretical data or conflicting in different sources; **Red:** No/insufficient data.

Figure 7. Status of the thermophysical properties of pure molten chlorides of interest in the MSR campaign and CsI. Melting temperatures of salts are also provided.*

4. CONCLUSIONS AND FUTURE WORK

Oak Ridge National Laboratory completed thermophysical characterizations of FLiNaK salt on three of the four measurement systems, including density, specific heat capacity, and thermal conductivity. The viscosity measurement system was calibrated and demonstrated with NIST-traceable standards and is ready for deployment on high-temperature salt mixtures. These collected data sets were compared to existing literature for validation and showed reasonable agreement with density and specific heat capacity data. Areas of improvement were identified for future work. The thermal conductivity data suggested potential negative trends with temperature, which is in agreement with modeling and theory but was not achievable using previous techniques. However, optical property data must be available to fully quantify the effects of radiative heat transfer.

Redlich-Kister (RK) expansion models were developed to provide a means for estimating thermophysical properties with varying composition and temperature. This modeling technique will enable analysis of other salt systems and wider ranges of temperatures not feasible with existing experimental techniques, and it will also identify knowledge gaps in existing data. As such, leveraging modeling can drive the design of future measurement campaigns, with the goal of reducing modeling uncertainty and filling in the identified

Salt	Density	Viscosity	Thermal conductivity	Heat Capacity	Melting T (°C)
AlF_3					1290
BaF_2					1368
BeF_2					548
CeF_3					1432
CeF_4					650
CrF_3					1404
CsF					703
FeF_2					970
KF					858
LiF					848
NaF					995
NdF_3					1377
NiF_2					1474
PuF_3					1426
SrF_2					1473
ThF_4					1110
UF_3					1495
UF_4					1036
ZrF_4					910

* **Green:** Experimentally supported or well-established; **Yellow:** Only theoretical data or conflicting in different sources; **Red:** No/insufficient data.

Figure 8. Status of the thermophysical properties of pure molten fluorides of interest in the MSR campaign, with melting temperatures of salts.*

knowledge gaps. This effort included collaboration with other national laboratories and universities to build the thermophysical and thermochemical databases. ORNL will continue to push the limitations of its characterization methods to enable the use of more salt systems of interest in the reactor developer community.

5. REFERENCES

[1] D. Hill, S. Cantor, and W. Ward, "Molar Volumes in the LiF–ThF *sub*4 System." Oak Ridge National Lab., Tenn., Tech. Rep., 1967.

[2] J. H. Shaffer, "Preparation and Handling of Salt Mixtures for the Molten Salt Reactor Experiment." Oak Ridge National Lab., Tenn., Tech. Rep., 1971.

[3] D. Sulejmanovic, J. M. Kurley, K. Robb, and S. Raiman, "Validating Modern Methods for Impurity Analysis in Fluoride Salts," *Journal of Nuclear Materials*, vol. 553, p. 152972, 2021.

[4] L. C. Olson, J. W. Ambrosek, K. Sridharan, M. H. Anderson, and T. R. Allen, "Materials Corrosion in Molten LiF–NaF–KF Salt," *Journal of Fluorine Chemistry*, vol. 130, no. 1, pp. 67–73, 2009.

[5] X.-H. An, J.-H. Cheng, T. Su, and P. Zhang, "Determination of Thermal Physical Properties of Alkali Fluoride/Carbonate Eutectic Molten Salt," in *AIP Conference Proceedings*, vol. 1850, no. 1. AIP Publishing LLC, 2017, p. 070001.

[6] M. Smirnov, V. Khokhlov, and E. Filatov, "Thermal Conductivity of Molten Alkali Halides and Their Mixtures," *Electrochimica acta*, vol. 32, no. 7, pp. 1019–1026, 1987.

[7] A. E. Gheribi and P. Chartrand, "Thermal Conductivity of Molten Salt Mixtures: Theoretical Model Supported by Equilibrium Molecular Dynamics Simulations," *The Journal of chemical physics*, vol. 144, no. 8, p. 084506, 2016.

[8] Y. Ishii, K. Sato, M. Salanne, P. A. Madden, and N. Ohtori, "Thermal Conductivity of Molten Alkali Metal Fluorides (LiF, NaF, KF) and Their Mixtures," *The Journal of Physical Chemistry B*, vol. 118, no. 12, pp. 3385–3391, 2014.

[9] C. D. Chliatzou, M. J. Assael, K. Antoniadis, M. L. Huber, and W. A. Wakeham, "Reference Correlations for the Thermal Conductivity of 13 Inorganic Molten Salts," *Journal of physical and chemical reference data*, vol. 47, no. 3, p. 033104, 2018.

[10] C. Jin-Hui, Z. Peng, A. Xue-Hui, W. Kun, Z. Yong, Y. Heng-Wei, and L. Zhong, "A device for measuring the density and liquidus temperature of molten fluorides for heat transfer and storage," *Chinese Physics Letters*, vol. 30, no. 12, p. 126501, 2013.

[11] K.-C. Chou and J.-H. Hu, "A New Experimental Method for Determining Liquid Density and Surface Tension," *Metallurgical Transactions B*, vol. 22, no. 1, pp. 27–31, 1991.

[12] M. Rose, "Thermophysical Property Measurements: Improved Density, Viscosity and Thermal Diffusivity Methods," no. ANL:CFCT-20/38.

[13] S. Cohen and T. Jones, "A Summary of Density Measurements on Molten Fluoride Mixtures and a Correlation for Predicting Densities of Fluoride Mixtures," Oak Ridge National Lab., Tenn., Tech. Rep., 1954.

[14] J. Cibulková, M. Chrenková, R. Vasiljev, V. Kremenetsky, and M. Boca, "Density and Viscosity of the (LiF+ NaF+ KF) eut (1)+ K2TaF7 (2)+ Ta2O5 (3) Melts," *Journal of Chemical & Engineering Data*, vol. 51, no. 3, pp. 984–987, 2006.

[15] M. Chrenkova, V. Daněk, A. Silnỳ, V. Kremenetsky, and E. Polyakov, "Density and Viscosity of the (LiF NaF KF) eut KBD4 B2O3 melts," *Journal of molecular liquids*, vol. 102, no. 1-3, pp. 213–226, 2003.

[16] G. Mellors and S. Senderoff, "The Density and Surface Tension of Molten Fluorides," in *Electrochemistry*. Elsevier, 1965, pp. 578–598.

[17] G. J. Janz and R. Tomkins, "Physical Properties Data Compilations Relevant to Energy Storage. IV. Molten Salts: Data on Additional Single and Multi-Component Salt Systems," National Standard Reference Data System, Tech. Rep., 1981.

[18] N. D. B. Ezell, R. Gallagher, N. Russell, A. Martin, A. McAlister, and J. McMurray, "Thermophysical Property Measurements of Salt Mixtures," 2020.

[19] D. J. Rogers, T. Yoko, and G. J. Janz, "Fusion Properties and Heat Capacities of the Eutectic Lithium Fluoride-Sodium Fluoride-Potassium Fluoride Melt," *Journal of Chemical and Engineering Data*, vol. 27, no. 3, pp. 366–367, 1982.

[20] J. Ard, K. Johnson, M. Christian, J. Yingling, T. M. Besmann, J. W. Mcmurray, J. Peng *et al.*, "FY20 Status report on the Molten Salt Thermodynamic Database (MSTDB) development," Oak Ridge National Lab.(ORNL), Oak Ridge, TN (United States), Tech. Rep., 2020.

[21] J. W. McMurray, K. Johnson, C. Agca, B. R. Betzler, D. J. Kropaczek, T. M. Besmann, D. Andersson, and N. Ezell, "Roadmap for Thermal Property Measurements of Molten Salt Reactor Systems," Oak Ridge National Lab.(ORNL), Oak Ridge, TN (United States), Tech. Rep., 2021.

[22] O. Redlich and A. Kister, "Algebraic Representation of Thermodynamic Properties and the Classification of Solutions," *Industrial & Engineering Chemistry*, vol. 40, no. 2, pp. 345–348, 1948.

[23] J. W. McMurray and T. M. Besmann, "Thermodynamic Modeling of Nuclear Fuel Materials," *Handbook of Materials Modeling: Applications: Current and Emerging Materials*, pp. 2335–2363, 2020.

[24] U. R. Kattner, "The Thermodynamic Modeling of Multicomponent Phase Equilibria," *Jom*, vol. 49, no. 12, pp. 14–19, 1997.

[25] C.-A. Hwang, J. C. Holste, K. R. Hall, and G. A. Mansoori, "A Simple Relation to Predict or to Correlate the Excess Functions of Multicomponent Mixtures," *Fluid Phase Equilibria*, vol. 62, no. 3, pp. 173–189, 1991.

[26] P. Chartrand and A. D. Pelton, "Thermodynamic Evaluation and Optimization of the LiF-NaF-KF-MgF 2-CaF 2 System Using the Modified Quasi-Chemical Model," *Metallurgical and Materials Transactions A*, vol. 32, no. 6, pp. 1385–1396, 2001.

[27] Y.-M. Muggianu *et al.*, "Enthalpies de Formation des Alliages Liquides Bismuth-Étain-Gallium à 723 K. Choix d'Une Représentation Analytique des Grandeurs d'Excès Intégrales et Partielles de Mélange," 1975.

[28] C. Agca and J. W. McMurray, "Empirical Estimation of Densities in NaCl-KCl-UCl3 and NaCl-KCl-YCl3 Molten Salts Using Redlich-Kister Expansion," *Chemical Engineering Science*, p. 117086, 2021.